Developing the Multiple Stress-Strain Creep Recovery (MSSCR) Test

Mahmoud Elnasri, Gordon Airey and Nick Thom

Nottingham Transportation Engineering Centre, The University of Nottingham, University Park, Nottingham, NG7 2RD, UK

Mahmoud Elnasri (Corresponding author)
mahmoud.elnasri@outlook.com,

Abstract

While most published work from Europe has been concerned with evaluating binders' resistance to rutting based on their stiffness (deformation resistance), work originating in the US has mainly been concerned with ranking binders based on their recoverability in a multiple stress form. This paper details the design of a new modified multiple stress-strain creep recovery (MS-SCR) test. The test is designed to evaluate binders' rutting resistance based on two rutting resistance mechanisms: stiffness and recoverability. A preliminary investigation is presented in this paper followed by details of the design of the new modified test. A 40/60 penetration grade bitumen and bitumen-filler mastics prepared with three filler concentrations (35%, 50%, and 65% filler content by mass of mastic) were tested. In addition, two polymer modified bitumens (PMBs) using the same base bitumen type were examined for validation. Two parameters are introduced to characterise the short and long recovery in the new test. In terms of stiffness, the test allows the behaviour of binders at different stress levels and loading cycles to be studied and produces a new parameter that can quantify the degree of modification. Finally, a relationship between nonlinearity and normal force in the test was investigated.

Keywords *Bitumen; rutting; multiple stress creep recovery test*

1. Introduction

The resistance of an asphalt mixture to permanent deformation (rutting) is highly dependent on the properties of its binder. Previously, empirical tests (i.e. penetration and softening point) were used to evaluate the resistance of the binder to rutting. More recently, this evaluation has shifted from empirical to more fundamental rheological tests using the dynamic shear rheometer (DSR) to attain detailed characterisation and specific permanent deformation results. Nowadays, different rheological testing protocols and parameters are being developed to meet the demand for correct bitumen rutting evaluation methods.

The failure of the first rheological Superpave permanent deformation evaluation parameter (G*/sin δ), particularly with regard to polymer modified bitumens (PMBs), increased the awareness of the need for a more appropriate testing procedure and parameter. The G*/sin δ parameter was found to be unable to distinguish between successful modifiers and those which don't add value in terms of rutting resistance. A detailed review of problems associated with G*/sin δ can be found in (Delgadillo et al., 2006b), summarised as follows:

- The applied loading during the test is fully reversible which does not simulate the actual loading in the real pavement (real loading reaches a maximum and then returns to the zero level).
- The Superpave Parameter is calculated from the total dissipated energy during the loading cycle. The delayed elastic component of the total dissipated energy doesn't contribute to rutting (recoverable).
- The number of loading cycles in the test is not sufficient to reach steady state behaviour and thus to accurately characterise the bitumen resistance to rutting.
- The methodology of taking into account high volume of traffic and low speed by shifiting the grade of the bitumen to a higher pavement temperature is irrational. This is because modified binders' sensitivity to temperature and loading is different to that of a pure (unmodified) bitumen.

Commented [TN1]: I don't understand this sentence. If something reaches a maximum and then returns to zero that is the same as fully reversible to me

Commented [ME2R1]: Reversible means that during the test a force is applied in the DSR in the clockwise direction to a point and then also applies a force in the reversible direction (anticlockwise). In real pavements, the loading is applied to a point but then the material is allowed to recover by itself without a force (force-free during recovery).

Bahia et al. (2001), who addressed these issues, proposed the repeated creep recovery (RCR) test. The test is performed in the DSR by applying 300 Pa shear stress of 100 cycles comprising 1 s loading and 9 s unloading. The number of cycles was designated to reach the steady state condition and 300 Pa shear stress was selected to maintain the behaviour in the linear response region. However, the RCR is unsatisfactory as the 300 Pa applied stress in the RCR test is below the estimated stresses in a real pavement (Delgadillo et al., 2006a). In addition, binders experience strains estimated to be 0 to 500 times the overall mixture strain as suggested by (Drakos et al., 2001). However, determining the strain/stress that the binder is subjected to in the mixture is not easy. An alternative approach would be to apply different stress levels so that the binder behaviour can be captured over a wider range.

Recent advancement of the creep-recovery test introduced the multiple stress creep recovery (MSCR) test. The test comprises 10 sequential cycles of 1 s loading and 9 s unloading repeated at 11 stress levels in an ascending order. It is widely recognised as a more accurate indicator to rank binder (pure or modified) in terms of rutting, is simple and easy to perform, and well correlated to asphalt mixture rutting performance (D'Angelo et al., 2007; Zoorob et al., 2012; D'Angelo, 2010; Wasage et al., 2011). Temperature, which has a significant impact in asphalt mixtures' rutting resistance (Qiao et al., 2013), is selected in the MSCR test based on the binder type. Binders in the MSCR test are evaluated and ranked based on their recoverability.

In Europe, attention has focussed on a parameter termed Zero-Shear-Viscosity (ZSV) to evaluate rutting resistance of binders (Giuliani et al., 2006; Morea et al., 2010; Vlachovicova et al., 2007). The ZSV in principle is a measure of the deformation resistance 'stiffness' of a material. The concept of ZSV emerged based on the assumption that only linear viscoelastic behaviour occurs under wheel loading in rational pavement design. At this 'steady state' condition bitumen deforms slowly without any change in the structure with the colloidal system maintaining an equilibrium state. The corresponding viscosity at this stage (ZSV) is independent of the shear rate and is an intrinsic property of a binder to evaluate deformation resistance.

Various testing methods have been used to determine ZSV ranging from creep, creep-recovery to oscillation and viscometry (Desmazes et al., 2000; De Visscher and Vanelstraete, 2004; Giuliani et al., 2006). In addition, ZSV can be extrapolated through mathematical models (Biro et al., 2009; Le Hir et al., 2003; Anderson et al., 2002; Liao and Chen, 2011). Different test methods (different loading and recovery times, stress levels and temperatures) have been suggested to fit different binder types.

For instance, Morea et al. (2010) performed 1 and 4 hr creep loading on pure and modified bitumen respectively to calculate the ZSV within the last 15 minutes. When the steady state condition was not reached, the loading was continued for a further 4 hrs and, whether the steady state was reached or not, the ZSV was then calculated. Giuliani et al., (2006) found that for binder with high rubber content (4%), the steady state could not be reached using the 4 hrs and 15 minutes testing protocol. Using a frequency sweep test, Giuliani et al., (2006) tested binders over a frequency range of 1 to 10 Hz. On the other hand, Biro et al., (2009) used decades of frequencies [0.01 – 0.10], [0.1 - 1],[1 , 10] to examine warm asphalt binders.

It is difficult to find a general agreement on the best testing method or condition to measure ZSV as different binders with different stiffness require different testing conditions. Changing the test condition (temperature, stress level, loading time) is therefore required to fit different types of binder with different stiffness. This is understandable as when the binder is stiff enough, the zero level of steady state is either not reached or requires impractical waiting times.

The literature presented above reveals that binders are ranked against rutting either by their recoverability (MSCR) or stiffness. MSCR can rank binders only based on their recoverability while some binders (as will be detailed later) have a high stiffness and low recoverability. On the other hand, there is no general agreement on a testing method that can suit all binder types when measuring their stiffness or ZSV.

The objective of the paper is to design a new Multiple Stress-Strain Creep Recovery (MS-SCR) test, able to distinguish between the two rutting resistance mechanisms; stiffening (deformation resistance) and recoverability which can fit all binder types. Binder herein refers to either pure bitumen, mastic (bitumen + filler), or PMB. Traditional 40/60 pen bitumen and mastics using the same base bitumen with limestone at three different concentrations (35%, 50%, and 65% filler content by mass of mastic) were tested. In addition, two PMBs using the same base bitumen type were examined to validate the effectiveness of the test.

Initially, a preliminary investigation was undertaken to characterise the recovery property of the different binders. Then, the standard MSCR test was run on the different binders. After that, the development of the MS-SCR is discussed followed by the experimental results and discussion. Finally, the outcomes of the paper are summarised in the last section.

2. Experimental programme

2.1 Materials

A typical 40/60 pen bitumen ‘B’ (with 40 dmm penetration and 53.8^{0}C softening point according to BS EN 2000-49:2007 and BS EN 2000-58:2007 respectively) widely used in UK road construction and supplied by Nynas Bitumen was employed as the base bitumen for this study. Limestone filler (passing sieve No. 230) was blended with the 40/60 bitumen at three filler concentrations: 35%, 50%, and 65% by mass of mastic, designated here as M35, M50, and M65 respectively. The 35% and 65% mastics correspond to the lower and upper limits respectively of filler content in a 10 mm DBM (BS EN 4987-1:2005) with 50% being used as a midpoint representing practical mixtures. In addition, two polymer modifiers, elastomer SBS and plastomer EVA, were mixed with the same base bitumen (designated P1 and P2 respectively) at 5% content by total PMB mass.

To ensure accurate measurements, a very precise procedure was followed to prepare representative mastic samples. Initially, bitumen and filler were heated at 160^{0}C and 105^{0}C respectively before the correct amount of filler was added in small portions to the heated bitumen. Continuous and gentle manual stirring was applied during mixing to achieve a homogenous state and avoid lump formation. Similarly, polymer was added in small amounts to the heated bitumen with continuous blending through a mechanical shear mixer. The hot mastic and PMBs were then distributed into 10 mm vials, left to cool and then stored at 5^{0}C for further testing. From visible inspection, incompatibility was observed with P1 (SBS polymer). Nevertheless, preparation was continued to examine the ability of the MS-SCR to recognise how well the blending with polymer has taken place in a PMB.

2.2 Test equipment and sample preparation

A calibrated Kinexus DSR type from Malvern® with a torque limit up to 0.2 N.m and fitted with a rapid environmental controller (-40 to 200^{0}C) was employed as shown in Figure 1. In comparison to the old generation DSR, the machine software offers high flexibility to customise a required test with precise resolution (0.1 nNm torque resolution and 0.001^{0}C temperature accuracy). In addition, temperature is controlled by air to avoid any possible de-

Commented [TN3]: You mean nanoNewton??

Commented [ME4R3]: Yes

bonding between sample and plates due to the use of a liquid temperature control system. 25 mm diameter parallel plates with 1 mm gap geometry were used for all testing.

Fig. 1 Kinexus DSR type

Accurate sample preparation is a central requirement for accurate rheological measurements as results are sensitive to sample geometry. The 'hot pour' method was applied as recommended to attain maximum repeatability and consistency (Airey and Hunter, 2003). Initially, vials were heated for 15 minutes at 180^0C for the PMBs and 160^0C for the pure bitumen and mastics while the plates were kept at 60^0C to accomplish sufficient adhesion. After raising the upper plate from the zero-gap setting, a sufficient amount of the binder was poured onto the centre of the lower plate. The gap was closed to reach a height of 1.05 mm after which the sample was carefully trimmed around the circumference to remove surplus material. Finally, the gap was lowered to 1.00 mm and the active hood was closed on the Kinexus to allow 15 minutes thermal equilibrium time after reaching the target testing temperature.

2.3 Preliminary tests

To characterise the recovery property of the binders, single creep-recovery tests were performed. The test was implemented on neat bitumen and mastics at 1 and 10 kPa shear stress at both 30 and 50^0C. For each test, a constant load was applied to reach a target strain and then the load was removed. Measurements of strain were continuously recorded during the unloading phase until an approximately constant strain level (no more recovery) was reached. The test was repeated for each binder with different loading times (to reach different strain levels) to observe the relationship between the loading strain and the recovered strain at different stress levels, temperatures and filler contents.

Secondly, the standard MSCR test was performed at 30, 40, and 50^0C on bitumen and mastics. At each stress level 10 cycles of 1 s loading and 9 s unloading were implemented. The average unrecovered strain divided by the associated shear stress yields the J_{nr}; the non-recoverable creep compliance, the evaluation parameter in the MSCR test. The J_{nr} parameter is an indicator of the resistance of an asphalt binder to permanent deformation under repeated creep.

2.4 Design of MS-SCR

The literature review above revealed that the MSCR test is the most recent advancement in terms of a rutting evaluation test for binders. Of the previous tests, it better represents field conditions, is easy and quick to perform, and with the 10 applied stress levels allows binder stress sensitivity to be assessed. Based on various observations related to the MSCR test, the following modifications to the test were applied as detailed in the subsequent points.

Observations of MSCR test

- The strain reached at each cycle varies depending on the material's stiffness. Consequently, different binders attain different strains at the same cycle and stress level. Preliminary investigation will reveal that the recovered strain is dependent on the loading strain at each stress level. Hence, different loading strains result in different recoveries.
- The strain varies in repeated cycles within one stress level. Although 10 cycles are performed, it requires around 50 cycles before a stable strain value is reached (Bahia et al., 2001; Golalipour, 2011).
- The 9 second recovery period is not satisfactory to fully release the stored delayed elastic strain, potentially affecting the following loadings and recoveries cumulatively.
- The MSCR ranks binders based on their recoverability. However, there is an inevitable requirement to recognize the other rutting resistance mechanism: the stiffening effect (deformation resistance) especially when the recoverability is low and the deformation resistance is high as in mastics.

Modifications associated with MS-SCR test

- Each stress is accompanied by a targeted strain limit to be repeatedly reached at each cycle, allowing the creep time to vary as necessary. Consequently, different binders will deform equally in terms of stress and strain but will vary their loading times depending on their stiffness. Different timings reflect different traffic conditions.
- A targeted fixed strain at each stress level repeated at each cycle eliminates the requirement of having a higher number of cycle repetitions to reach a stable strain value for all cycles.

- A 5 minutes recovery time is allowed at the 10^{th} cycle of each stress level which mitigates any delayed elastic effect between stresses and offers a comparison between short and long recovery behaviours.
- Two factors are introduced to distinguish between the stiffening effect and recoverability rutting resistance mechanisms.

The idea of targeting a fixed strain to be repeatedly reached at each cycle for each stress level is to establish a unified condition of testing so that results are comparable. The applied stresses and 9 s unloading time used in the standard MSCR are used in the MS-SCR. The corresponding strains in the MS-SCR, presented in Table 1, are derived based on initially finding the strain level that can be reached and not exceeded for all binder types at all testing temperatures within 1 s of loading. This was carried out on the neat bitumen (the softest binder) at 50^0C at 25 Pa and 25.6 kPa and the strain was found to be 0.58% and 350% respectively. As pure bitumen at 50^0C produced these strains for 1 s loading, the other stiffer binders (mastic and PMB) will not exceed these strains within 1 s loading at any testing temperature $\leq 50^0$C.

Secondly, a linear relationship was produced between the stresses and the strains. More specifically, a ratio of 1.89 between consecutive strains was selected to approximately produce a linear relationship of applied stress-strain (Figure 2). This will be used to examine any deviation from linearity caused by the nature of the binder (inherent nonlinearity). A schematic diagram presenting the MS-SCR test is shown in Figure 3.

Table 1 Applied stresses and their associated strains

Stress (Pa)	25	50	100	200	400	800	1600	3200	6400	12800	25600
Strain (%)	0.60	1.13	2.20	4.09	7.75	14.69	27.86	52.83	100.15	189.88	350.00

Fig. 2 Applied stress-strain plot in MS-SCR test

Fig. 3 Schematic diagram of MS-SCR test (not to scale)

3. Results and discussion

3.1 Preliminary Investigation

Single creep recovery tests were performed to observe the relationship between recovered strain and total strain taking into consideration the effect of temperature and stress level. Figure 4 combines typical responses at different loading and unloading times for mastic M50 at a stress of 1 kPa and 30°C. The trend shows a viscoelastic behaviour in which the strain is partially recovered after loading removal. Similar trends were observed for the other tested binders. Figures 5 and 6 summarise the final recovered strain versus total (applied) strain at 1 kPa and 10 kPa respectively.

Fig. 4 Creep recovery results of M50 @1 kPa and 30^0C

Fig. 5 Recovered strain behaviour of different binders @1 kPa

Fig. 6 Recovered strain behaviour of different binders @10 kPa

Similar to the previous findings of (Ossa et al., 2005), regardless of the stress, temperature and filler content, the total strain at relatively low strain levels (approximately less than 0.5) has a linear relationship with the recovered strain. After this at higher strains, the recovered strain becomes constant upon reaching a total strain level. It can be observed that the total strain level after which the recovered strain becomes constant is a function of the stress level and filler content and insignificantly influenced by temperature. As the stress level is increased and/or filler content is reduced the total strain after which the recovered strain becomes constant rises to a higher value.

3.2 MSCR results

Typical results of MSCR at 30^0C are presented in Fig 7. As can be observed from Fig. 7, as the filler content is increased in the binder, the deformation (strain) in the binder decreases due to the increased stiffness of the mastic. However, the inserted plot in Fig.7 also shows that although B has larger deformation (strain), it has higher recovery than the other binders.

Fig. 7. Typical result of MSCR test at 30^0C

It was also noted by (Mturi et al., 2012) that the strain for a constant applied stress increases after each successive loading cycle. The strain (non-accumulated) at the end of each cycle was therefore investigated. Figure 8 shows the coefficient of variation (CoV) of these strains at each stress level at 30, 40, and 50^{0}C which confirms the finding of variability in attained strains for the different cycles.

Fig. 8. CoV of strains versus stress level in MSCR test

As the resulting strain is not constant for successive cycles at each stress level in the MSCR test, and considering the results from the previous single creep recovery test, the recovered strain will not be the same for different binders tested using the MSCR procedure. Mturi et al., (2012) also showed that for certain PMBs there is an increase in their unrecovered strain with increasing number of cycles while for others there is a decrease when testing these binders in the MSCR test. Therefore, the averaging approach of J_{nr} may not hold as it does not reflect the change in strain with cycle repetition or stress increase.

3.3 MS-SCR Results

The MS-SCR test was performed at 30, 40 and 50°C on the neat bitumen, two PMBs and mastics of three filler contents (35%, 50%, and 65% by mass). Representative results for the MS-SCR test at 40°C are shown in Figure 9 which shows accumulated strain against time. The results illustrate that there are variations in the loading times as well as discrepancies in the accumulated strains depending respectively on the stiffness and recoverability of the binder type. In addition, for each binder type, the variation and discrepancy apply between different cycles at one stress level.

Fig. 9 Typical results of MS-SCR @40^{0}C

A closer comparison of strain versus time for cycle 1 (C1) and cycle 9 (C9) at 40°C is illustrated in Figure 10. Dotted lines at 25 Pa are plotted against the left Y-axis while full lines of 1600 Pa follow the secondary Y-axis. All binder types follow the same pattern of loading and unloading and reach the same strain level at the same testing stress.

Fig. 10 Loading and recovery of different cycles @40^{0}C

It can be observed that for the same cycle and stress/strain level, the amount of loading time and recovery level vary between binder types depending on their stiffness and recoverability respectively. For example, at 1600 Pa M65 requires more time than P2 and B for C1 and C9, while P2 shows more recovery than M65 and B. Also at one stress level, each binder type has different loading times and different recoveries between different cycles due to the binder's loading/unloading history. For instance, C9 of M65 at 1600 Pa requires a longer loading time than that required for C1.

The MS-SCR test addresses both deformation resistance and recoverability for different cycles and stress levels. Further investigation of creep loading and recovery of different binders with the MS-SCR test are discussed in the following sections.

Average short and long recoveries:

The preliminary testing results revealed that the recovery maintains a constant value after reaching a strain limit. It is interesting to re-observe the recovery behaviour in the MS-SCR test. Figure 11 shows the recovered strain against the total strain. Similar to the preliminary results, different binders show different recoveries and increasing the stress/strain values increases the recovered strain. The same trend can be observed in the standard MSCR test; however, the total accumulated strain in the MSCR is not equal for all binders as in the MS-SCR test.

It can be seen from Fig. 11 that while P2 extensively shows high recoverability in comparison to the other binders, P1 has low recoverability (even lower than B) due to the polymer-bitumen incompatibility as previously noted. Moreover, the short recovered strain of P2 at each stress level continues to increase with each repeated cycle before reaching a constant value. Therefore, averaging the recovered (or unrecovered) strain does not always provide an accurate representation of the true material behaviour. Finally, the long recovery at the last cycle of each stress level is as expected greater than the short recovery due to the difference in the allowed time to recover.

Fig. 11 Recovered strain and total strain @40^{0}C in MS-SCR

Similar to J_{nr} in MSCR, two parameters are introduced to characterise the recovery; the average short and long recoveries. They are defined respectively as the average recovered strain of the first 9 cycles and the longer time recovered strain of the last cycle (cycle 10) both divided by the corresponding stress. Mathematically expressed by:

$$R_{ns} = {\sum_{i=1}^{9} R_i}\Big/{9\ \tau_m} \qquad (3)$$

$$R_{nl} = {R_{10}}\big/{\tau_m} \qquad (4)$$

Where R_{ns} is the average short recovered strain for stress level τ_m, R_i is the recovered strain at cycle i, R_{nl} is the long recovered strain at stress level τ_m, R_{10} is the recovered strain at cycle 10, and τ_m is the shear stress that varies from 25 Pa to 25.6 kPa.

Presentations of the two parameters at 30 and 50^0C are shown in Figures 12 and 13 respectively. The results demonstrate that both recovered strains follow approximately the same trend of a constant level before they start to reduce gradually. Also, the greater the temperature and/or filler content, the shorter is the constant recovery stage. Long recoveries are always higher than short recoveries due to the longer time allowed to recover.

Fig. 12 Average recoveries @30^0C
Fig. 13Average recoveries @50^0C

Cycle and stress loading behaviour

Both filler and polymer stiffened the bitumen by increasing the required loading time. However, it can be observed from Figures 5 and 6 that the recovery property of the mastic is reduced by filler inclusion. Therefore, a second factor is required to distinguish between the two mechanisms of rutting resistance. The notion of a stiffening factor was derived through the concept of mechanical modelling.

For viscoelastic materials those models comprise physical elements such as springs and dashpots combined to simulate the behaviour (Woldekidan, 2011). In the time-domain, creep loading that represents increased deformation with time under constant loading is extensively simulated by means of the Burger's model as represented in Figure 14. The model incorporates retardation time which describes the rate of strain growth over a certain time period. A lower rate of strain growth is an indication of higher resistance. After the instantaneous elastic deformation upon load application, the loading time to reach a specific strain value can represent a comparison factor of a material stiffness.

Fig. 14 Burger's model and viscoelastic behaviour

In the MS-SCR test, the strain and stress levels are constants at each cycle but loading time varies depending on the material stiffness (Figure 9) and can be employed to quantify the deformation resistance. Two features associated with creep loading time are identified; the change of creep cycle time at one stress level (cycle loading time), and creep time change with stress increase (normalised creep time).

Cycle loading behaviour

The creep cycle time is defined as the loading time required to reach the target strain at each cycle. Figures 15 and 16 show a comparison of the creep cycle loading time between the 1st cycle and the last (10th) cycle at 30, 40 and 50^{0}C for B, P2 and M65 at each stress level. As can be seen, there is no difference in the consumed time between C1 and C10 for both M65 and B. P2 on the other hand required more time for C10 than C1. The delayed elastic effect due to insufficient recovery time is perceived to be the cause of the difference in P2. It can be noticed that while B and P2 gradually reduced their loading time with increasing stress level, M65 slightly increased and then decreased its loading time with increasing stress level. This could hypothetically be due to the high content of filler in M65 that requires a stage of filler particle structural-orientation before reaching full particle-particle contact resistance.

Fig. 15 Loading time behaviour of cycle 1 and 10 for P2 and B
Fig. 16 Loading time behaviour of cycle 1 and 10 of M65

Stress loading behaviour

To measure the stiffening effect of modifier (either polymer or filler) with respect to stress change, the maximum normalised creep timing 'NCT' is introduced. The ratio of modified bitumen maximum creep time within the 10 cycles over the pure bitumen maximum creep time at the same stress level and temperature produces the NCT (pseudo stiffening effect parameter). The normalization measures the stiffening introduced by modification where the thermo-rheological interaction is taken into consideration. Mathematically it is given by

$$\text{NCT}={\max(T_m^{\tau_i})}\Big/{\max(T_B^{\tau_i})} \tag{5}$$

Where: $T_m^{\tau_i}$ and $T_B^{\tau_i}$ are the maximum creep times of the 10 cycles at stress level τ_i of the modified and pure bitumen respectively.

Figure 17 plots the comparison between NCT and stress level for mastics. As can be seen, the stiffening increases with increasing filler content and/or reducing temperature. While low and intermediate filler contents demonstrate almost constant values across the stress levels at one temperature, mastic with high filler (65%) content displays a trend of initially increasing to reach a plateau region followed by a continuous decline. The trend is very distinct at low temperatures but less so at higher temperatures with the increase and decrease of the curve possibly being a sign of nonlinearity.

Fig. 17 NCT versus stress of mastics with 35%, 50%, and 65% filler contents

To check this hypothesis, the creep compliance $J_{(t)}$ (strain/stress of the first cycle at each stress level) is examined. The first cycle is chosen to reduce the influence of loading history through cycle repeating. Figure 18 compares the difference between the neat bitumen (B) and highly filler modified mastic (M65) at 40^{0}C.

Fig. 18 Creep compliance of first cycle change with time @40^{0}C for B and M65

There is no observable change in the $J_{(t)}$ versus time slope for B as a function of the different stresses. On the other hand, M65 presents three stages related to the slope of $J_{(t)}$ versus time; a reduction of the slope between 25 to 400 Pa, a constant slope (400 to 1600 Pa), and finally an increase in slope (above 1600 Pa). These three stages as a function of stress level are typical of the relationship observed with the NCT trend. The stage at which the $J_{(t)}$ slope remains constant is by definition an indication of linear behaviour (i.e., stress independency). The early nonlinearity can be postulated as the stage during which interlocking particle-particle contact becomes established. The source of the second nonlinearity stage at which NCT starts to decrease, with an increase of $J_{(t)}$ slope, will be discussed in the following section.

Similar to the filler modification, P2 in Figure 19 exhibits at 30^0C an initial increase at low stresses before it starts to decline, similar to the behaviour seen at 40 and 50^0C. As expected, P1 with polymer incompatibility shows insignificant stiffening with a constant value along all the stress levels. In a similar way to the fillers which require some time to establish particle to particle interlocking, P2 is perceived to form its molecular network initially in the first nonlinearity stage. An illustration of *J(t)* changing its slope with stress increase for P2 at 30^0C is presented in Figure 20. Similar to M65, the slope follows three stages of inclination change. The decrease of NCT at high stress levels at low temperature as described earlier is a second nonlinearity stage with the following section providing more investigation about the source of this nonlinearity.

Fig. 19 NCT of PMBs change with shear stress

Fig. 20 Creep compliance of first cycle change with time @40^0C for P2

4. Normal force (3D state of stress)

Although several studies have intensively used DSR equipment to characterise the binder linear and nonlinear viscoelastic properties, the attention to the actual source or cause of nonlinearity is poorly investigated. DSR machines control the gap to maintain the thickness of the sample during the test through an automated normal force. The normal force acts in combination with the torque required to shear the test specimen resulting in the creation of two perpendicular applied stresses which can potentially affect the material response. The application of the different forces (stresses) and measurements of the deformed sample are shown in Figure 21.

Fig. 21 Schematic diagram of forces acting on a DSR sample

A full recording of the normal force during the MS-SCR test is presented in Figure 22. As can be seen, the compression normal force varies between the MS-SCR applied shear stresses and between cycles. It increases during the loading phase and relaxes during the recovery stage. Therefore, only the creep loading phase is affected by the normal force. Mastics with low (35%) and intermediate (50%) filler contents have marginal differences in the normal force in comparison to the pure binder (B). However, the high filler content in M65 resulted in high normal force in comparison to the pure binder B. To study the effect of temperature change, Figure 23 (A&B) compares the maximum normal stress at each shear stress level at 30 and 50^0C.

Fig. 22 Change of normal force with time in MS-SCR @40^0C
Fig. 23 Normal stress against shear stress in MS-SCR test

As can be seen in Figure 23, there is a constant level of marginal normal stress up to a shear stress level of approximately 3.2 kPa after which it rises considerably. In addition, the normal stress increases more when reducing the temperature due to increased dilation rate. It has been shown that the development of the normal stress is an indication of the dilation of the sample (Motamed et al., 2012). Mastic with concentrated filler content produces higher normal stresses at all temperatures than pure bitumen.

Deshpande and Cebon, (1999) introduced the shear box analogy to study dilation or increase in the free volume of bituminous samples. This analogy states that as the shear creep loading increases, particles establish their packing by riding over each other which increases the thickness in the vertical direction (dilation). For M65 at 40^0C, the normal stress starts to increase at the stress level of 3.2 kPa which is identical to the stress level at which the *J(t)* slope starts to increase after the secondary constant slope stage in Figure 18. The same trend is obtained at 30 and 50^0C for M65 as well as P2. This is evidence of normal force shifting the behaviour of mastic with high filler content to a nonlinearity phase. This type of nonlinearity is referred to as an 'interaction nonlinearity' type. It indicates that due to the presence of other load components, normal force for instance, the material shear strain response changes (Motamed et al., 2012).

Finally, P2 produces considerably higher normal stresses in comparison to the other binders and its nonlinearity can be linked with the trend in NCT. The entanglement of the polymer network in P2 causes the normal force to be up to approximately six times higher than that seen for the high filler content mastic.

5. Conclusions

The literature review covered the process of developing binder rutting evaluation tests and parameters including the most recent MSCR test. Based on the provided observations, modifications in the MSCR test were introduced to develop the new MS-SCR test. The MS-SCR was designed to efficiently distinguish between the two rutting mechanisms; recoverability and stiffening. Important observations have been concluded from the results:

- The recoverability of the binder is dependent on the stress and strain levels. At one stress level, the recovered strain becomes constant after reaching a strain limit.
- The level of strain reached in the MSCR test is different between different cycles at one stress level, and is different between different binder types in the same cycle. Consequently, the recovered strains are different.
- The new MS-SCR test applies the same stress and strain levels at each cycle to unify the condition of testing. The new ‘strain’ approach, rather than traditional ‘stress’ approach, opens a new method to study material behaviour. However, further study is required to standardise the selection of the level of the strains.
- To mitigate the effect of insufficient recovery time, an extended period of 5 minutes is introduced between different stress levels in the MS-SCR test.
- Long and short recovery of different binders can be studied in the new test as well as the recovery level at each stress/strain level.
- The new test allows the binder behaviour to be investigated. The ‘delayed elastic’ effect significantly influences the cyclic behaviour (both loading and unloading stages) of PMBs at low temperature. Mastics of high filler concentrations demonstrate a different mechanism of a pre-interlocking stage that affects cyclic behaviour and is temperature independent.
- Examining the linearity in the MS-SCR test revealed two nonlinearity phases that are experienced by the modified binders. At the early stages of MS-SCR at low stress levels the nonlinearity is possibly triggered by the process of establishing full particle contact and the

formation of networks in highly concentrated filler mastics and PMBs respectively. The high normal force acting perpendicular to the high shear stress also generated a second nonlinearity for the material response, classified as ‘interaction nonlinearity’. Between the two nonlinear phases the range of stresses that correspond to the linear viscoelastic stage was relatively short.

In general, the new MS-SCR test has been shown to successfully separate the two permanent deformation resistance mechanisms and addresses some of the issues associated with the MSCR test. There are still some aspects to be considered such as the applied strain levels and testing temperature. Specification criteria are also required to be able to use this newly developed test to select good permanent deformation performing binders.

References

Airey, G. D. & Hunter, A. E. Dynamic mechanical testing of bitumen: sample preparation methods. Proceedings of the Institution of Civil Engineers-Transport, 2003. Thomas Telford Ltd, 85-92.

Anderson, D., Le Hir, Y., Planche, J.-P., Martin, D. & Shenoy, A. 2002. Zero shear viscosity of asphalt binders. Transportation Research Record: Journal of the Transportation Research Board, 54-62.

Bahia, H. U., Hanson, D., Zeng, M., Zhai, H., Khatri, M. & Anderson, R. 2001. Characterization of modified asphalt binders in superpave mix design.

Biro, S., Gandhi, T. & Amirkhanian, S. 2009. Determination of zero shear viscosity of warm asphalt binders. Construction and Building Materials, 23, 2080-2086.

D'angelo, J., Kluttz, R., Dongre, R. N., Stephens, K. & Zanzotto, L. 2007. Revision of the superpave high temperature binder specification: the multiple stress creep recovery test (With Discussion). Journal of the Association of Asphalt Paving Technologists, 76.

D’angelo, J. 2010. New high-temperature binder specification using multistress creep and recovery. Transportation Research Circular, n. E-C147, 1-13.

De Visscher, J. & Vanelstraete, A. 2004. Practical test methods for measuring the zero shear viscosity of bituminous binders. Materials and Structures, 37, 360-364.

Delgadillo, R., Cho, D. & Bahia, H. 2006a. Part 1: bituminous materials: nonlinearity of repeated creep and recovery binder test and relationship with mixture permanent deformation. Transportation Research Record: Journal of the Transportation Research Board, 3-11.

Delgadillo, R., Nam, K. & Bahia, H. 2006b. Why do we need to change G*/sinδ and how? Road materials and pavement design, 7, 7-27.

Deshpande, V. & Cebon, D. 1999. Steady-state constitutive relationship for idealised asphalt mixes. Mechanics of materials, 31, 271-287.

Desmazes, C., Lecomte, M., Lesueur, D. & Phillips, M. A protocol for reliable measurement of zero-shear-viscosity in order to evaluate the anti-rutting performance of binders. PROCEEDINGS OF THE PAPERS SUBMITTED FOR REVIEW AT 2ND EURASPHALT AND EUROBITUME CONGRESS, HELD 20-22 SEPTEMBER 2000, BARCELONA, SPAIN. BOOK 1-SESSION 1, 2000.

Drakos, C., Roque, R. & Birgisson, B. 2001. Effects of measured tire contact stresses on near-surface rutting. Transportation Research Record: Journal of the Transportation Research Board, 59-69.

Giuliani, F., Merusi, F. & Antunes, I. 2006. Creep flow behavior of asphalt rubber binder–the zero shear viscosity analysis. Proceedings of the Asphalt rubber.

Golalipour, A. 2011. Modification of multiple stress creep and recovery test procedure and usage in specification. University of Wisconsin–Madison.

Kavussi, A. & Hicks, R. 1997. Properties of bituminous mixtures containing different fillers. Journal of the Association of Asphalt Paving Technologists, 66.

Le Hir, Y., Anderson, D., Planche, J., Martin, D. & Partl, M. Rheological characterization of bituminous binder to predict pavement rutting. Sixth International RILEM Symposium on Performance Testing and Evaluation of Bituminous Materials, 2003. RILEM Publications SARL, 117-123.

Liao, M.-C. & Chen, J.-S. 2011. Zero shear viscosity of bitumen-filler mastics. Journal of Materials in Civil Engineering, 23, 1672-1680.

Morea, F., Agnusdei, J. & Zerbino, R. 2010. Comparison of methods for measuring zero shear viscosity in asphalts. Materials and structures, 43, 499-507.

Motamed, A., Bhasin, A. & Liechti, K. M. 2012. Interaction nonlinearity in asphalt binders. Mechanics of Time-Dependent Materials, 16, 145-167.

Mturi, G. A., Nkgapele, M. & O'connell, J. 2012. Creep recovery behaviour of bituminous binders-relevance to permanent deformation of asphalt pavements.

Ossa, E., Deshpande, V. & Cebon, D. 2005. Phenomenological model for monotonic and cyclic behavior of pure bitumen. Journal of materials in civil engineering, 17, 188-197.

Qiao, Y., Flintsch, G., Dawson, A. and Parry, T., 2013. Examining effects of climatic factors on flexible pavement performance and service life. Transportation Research Record: Journal of the Transportation Research Board, (2349), pp.100-107.

Vlachovicova, Z., Wekumbura, C., Stastna, J. & Zanzotto, L. 2007. Creep characteristics of asphalt modified by radial styrene–butadiene–styrene copolymer. Construction and Building Materials, 21, 567-577.

Wasage, T., Stastna, J. & Zanzotto, L. 2011. Rheological analysis of multi-stress creep recovery (MSCR) test. International Journal of Pavement Engineering, 12, 561-568.

Woldekidan, M. F. 2011. Response modelling of bitumen, bituminous mastic and mortar. TU Delft, Delft University of Technology.

Zoorob, S., Castro-Gomes, J., Oliveira, L. P. & O'connell, J. 2012. Investigating the multiple stress creep recovery bitumen characterisation test. Construction and Building Materials, 30, 734-745.

Fig. 1 Kinexus DSR type

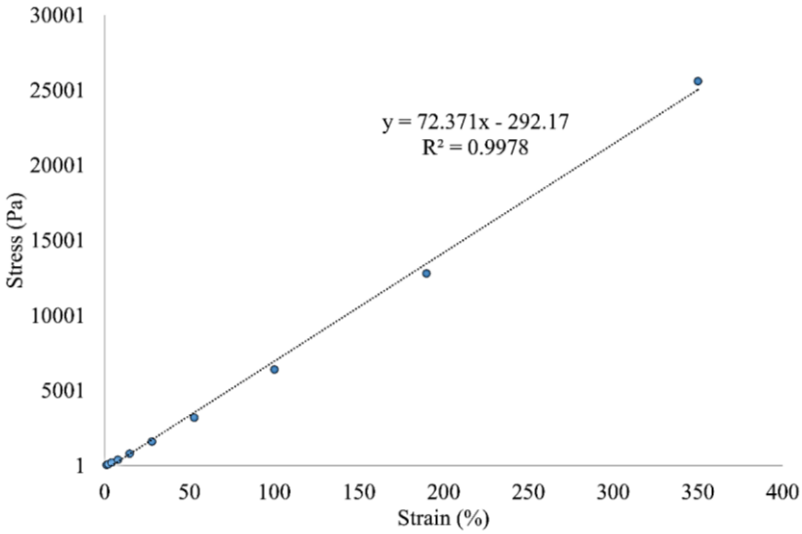

Fig. 2 Applied stress-strain plot in MS-SCR test

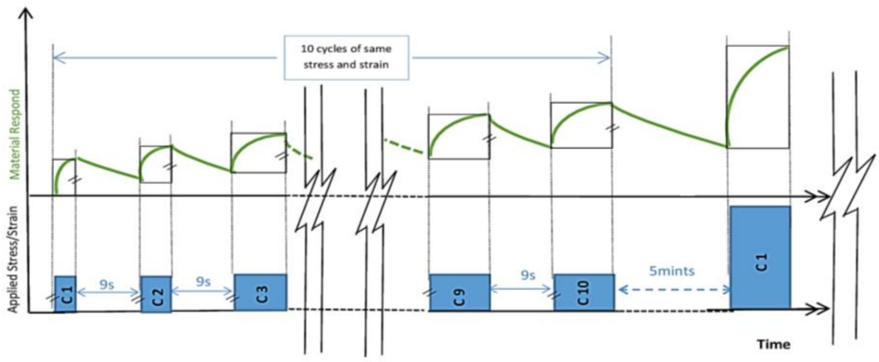

Fig. 3 Schematic diagram of MS-SCR test (not to scale)

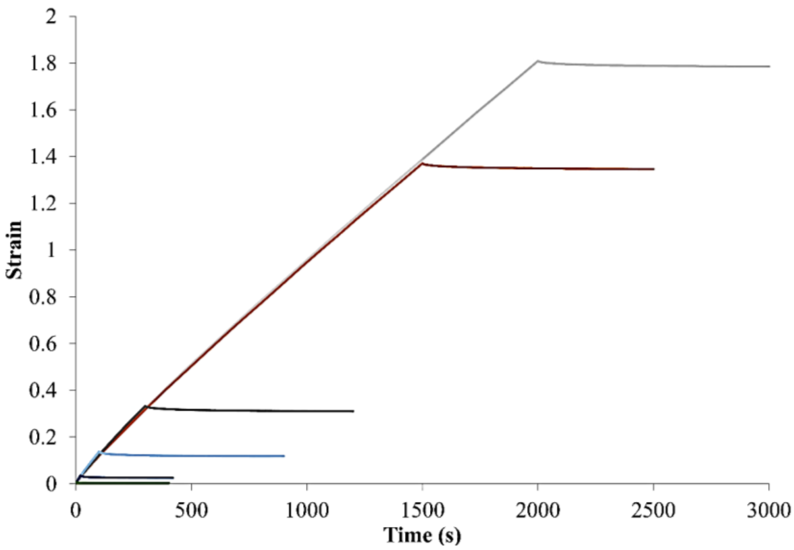

Fig. 4 Creep recovery results of M50 @1 kPa and 30^{0}C

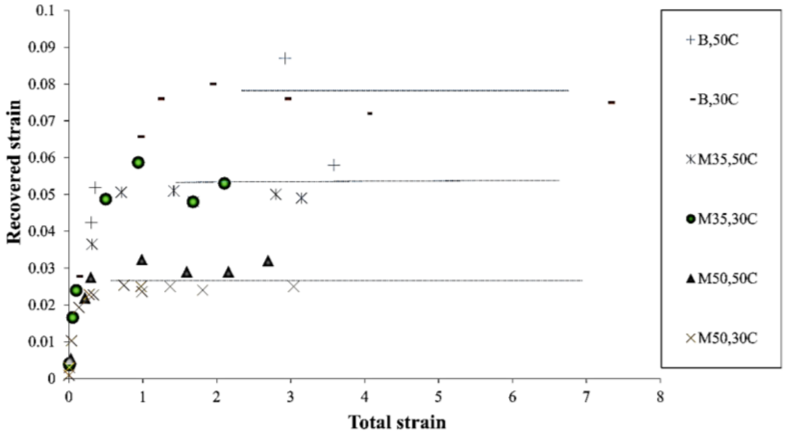

Fig. 5 Recovered strain behaviour of different binders @1 kPa

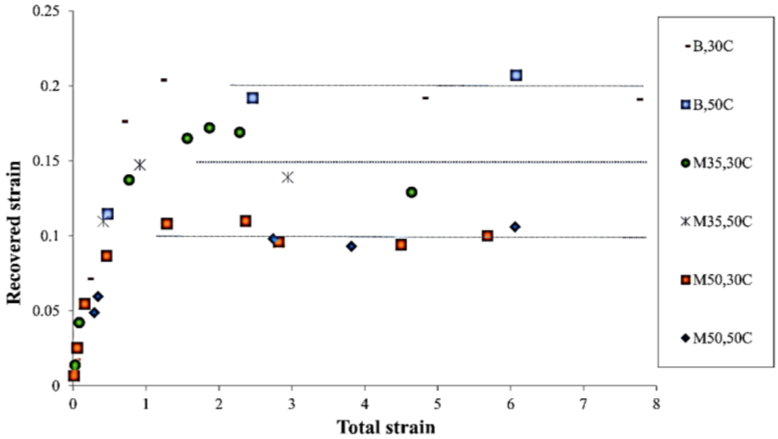

Fig. 6 Recovered strain behaviour of different binders @10 kPa

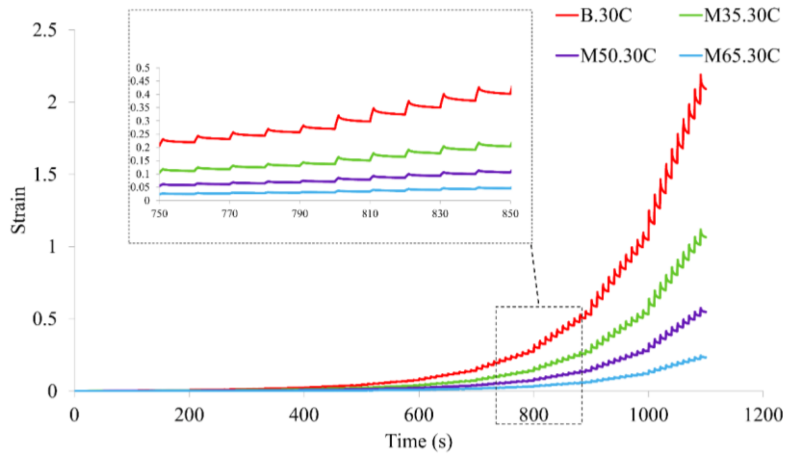

Fig. 7. Typical result of MSCR test at 30^0C

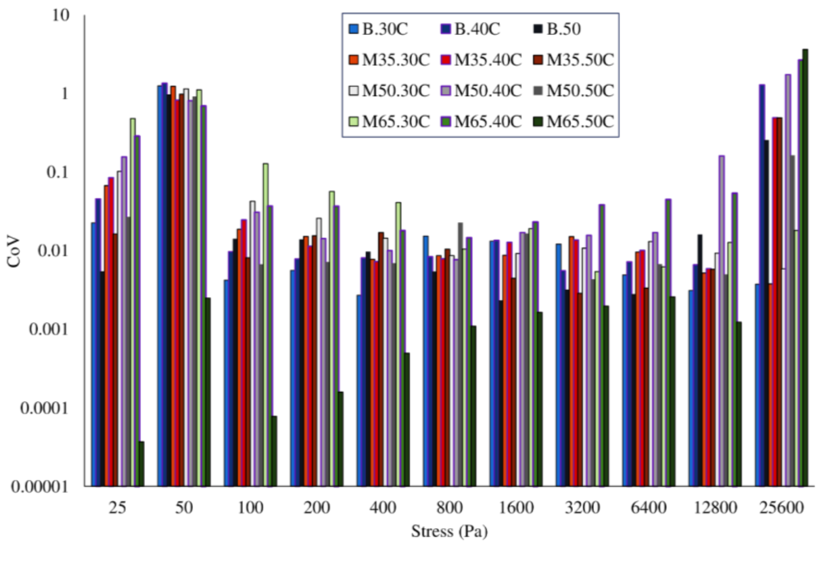

Fig. 8. CoV of strains versus stress level in MSCR test

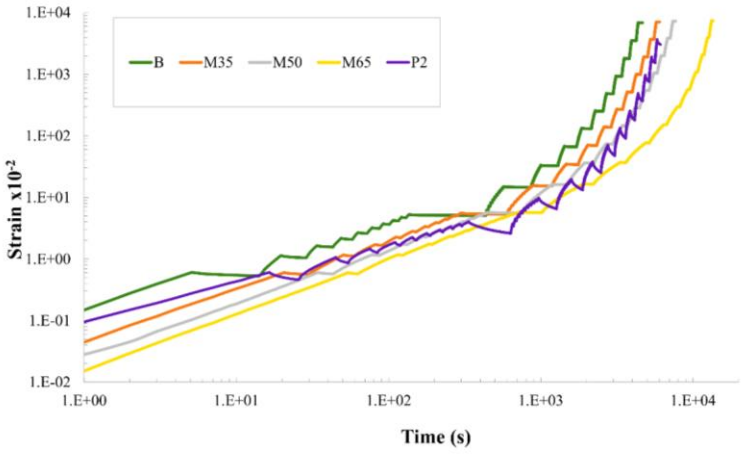

Fig. 9 Typical results of MS-SCR @40^{0}C

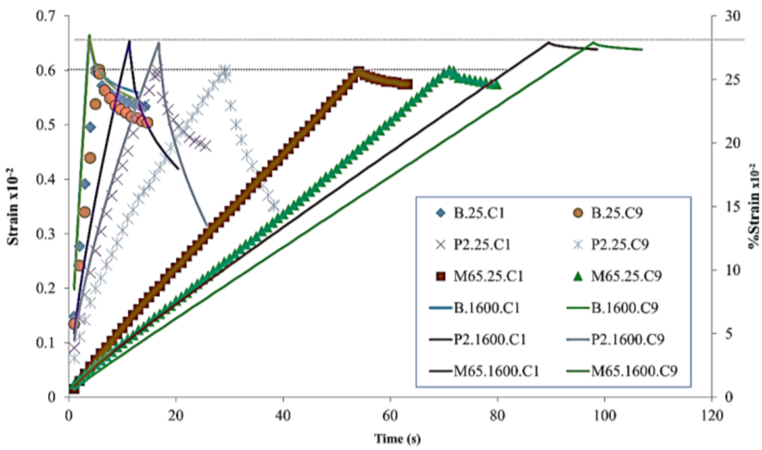

Fig. 10 Loading and recovery of different cycles @40^{0}C

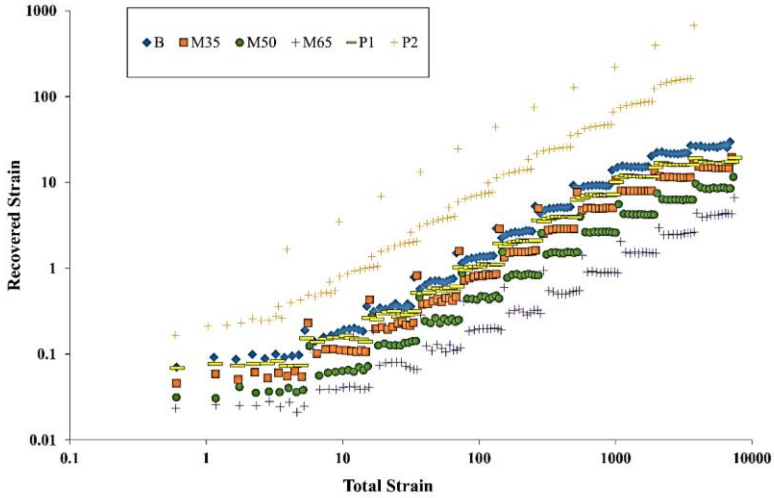

Fig. 11 Recovered strain and total strain @40^{0}C in MS-SCR

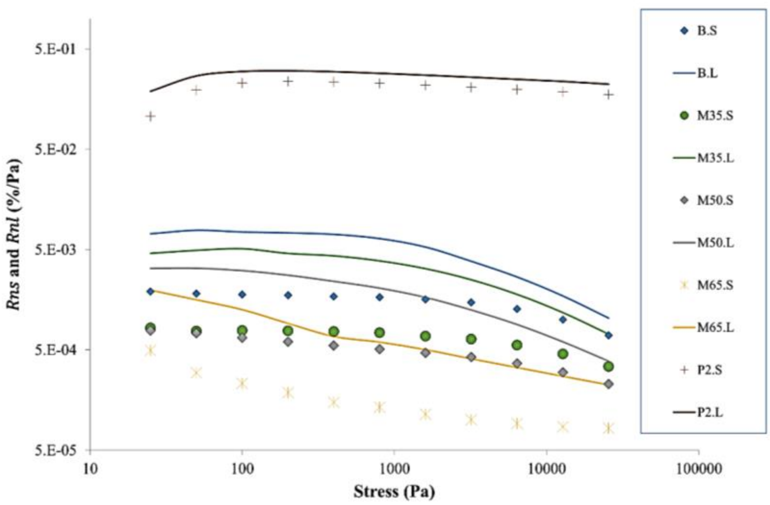

Fig. 12 Average recoveries @30^{0}C

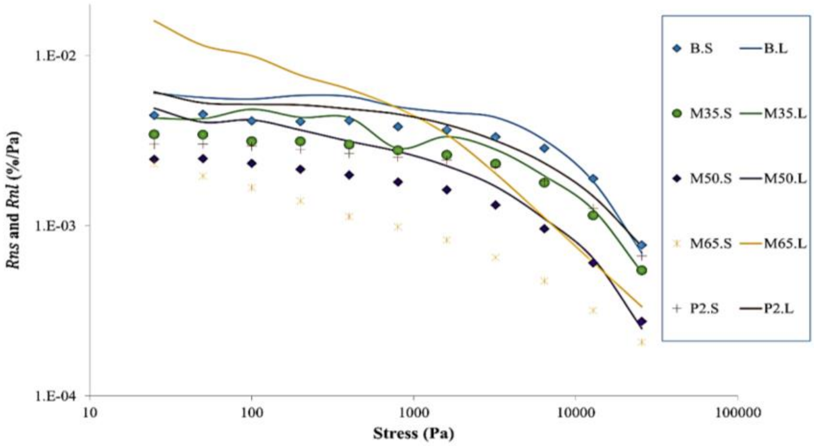

Fig. 13 Average recoveries @50^0C

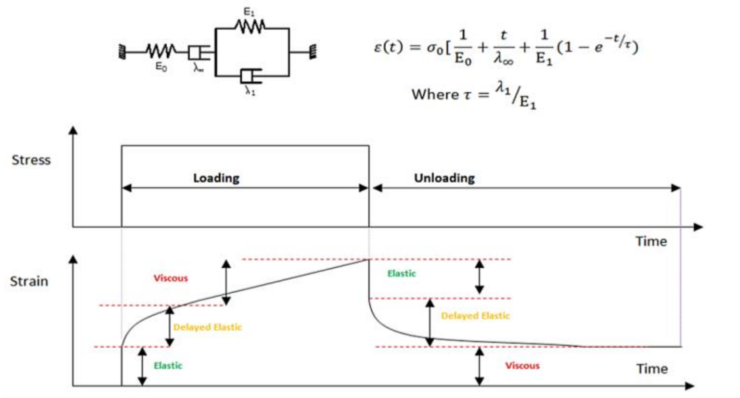

Fig. 14 Burger's model and viscoelastic behaviour

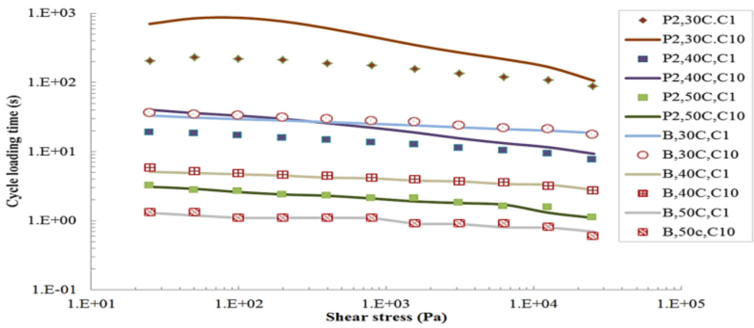

Fig. 15 Loading time behaviour of cycle 1 and 10 of P2 and B

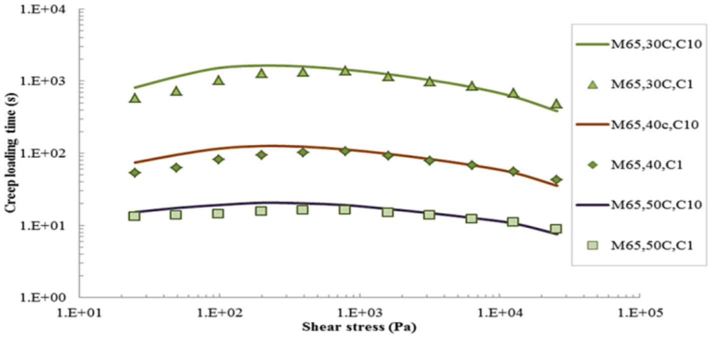

Fig. 16 Loading time behaviour of cycle 1 and 10 of M65

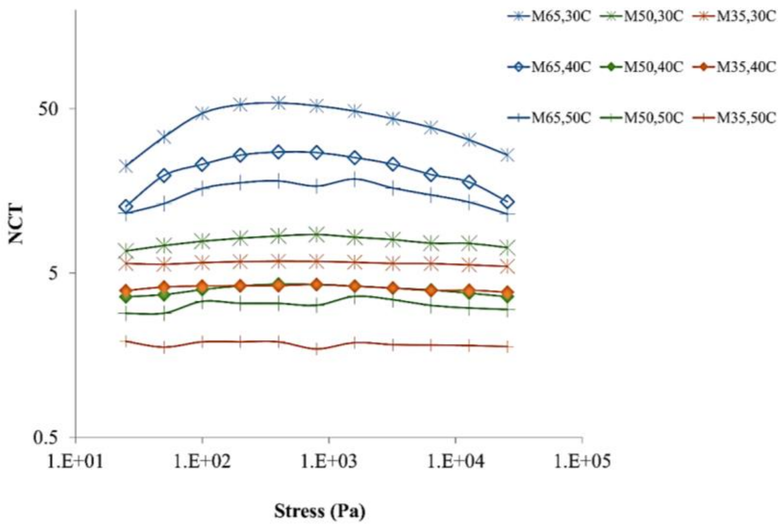

Fig. 17 NCT versus stress of mastics with 35%, 50%, and 65% filler contents

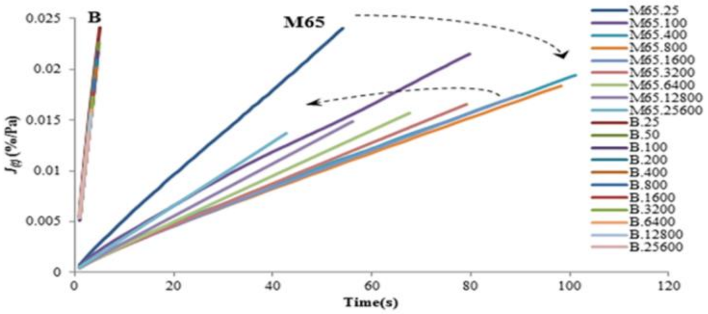

Fig. 18 Creep compliance of first cycle change with time @40^{0}C for B and M65

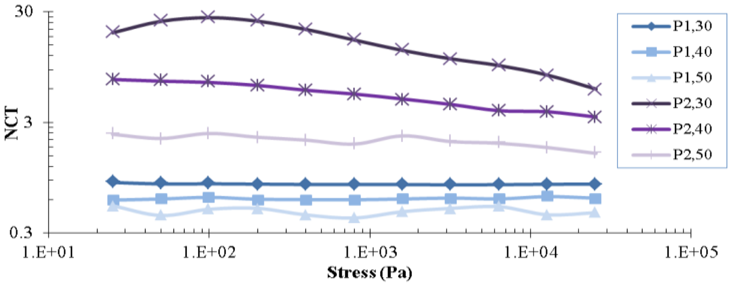

Fig. 19 NCT of P2 & P1 against shear stress

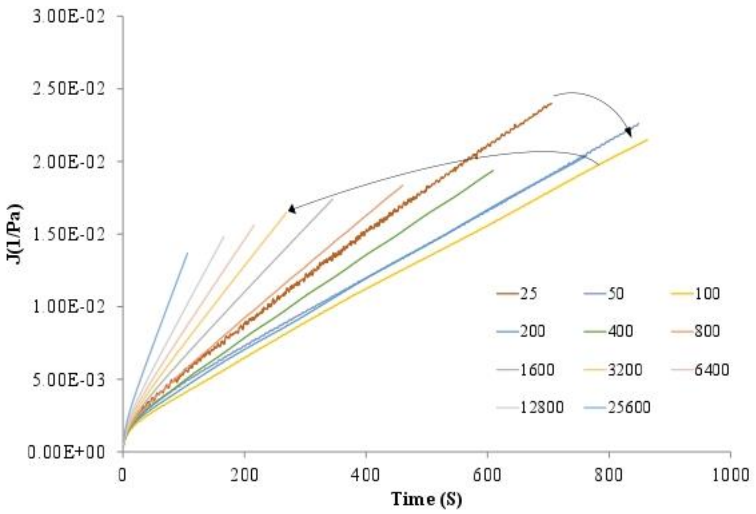

Fig. 20 Creep compliance of first cycle change with time @40^{0}C for P2

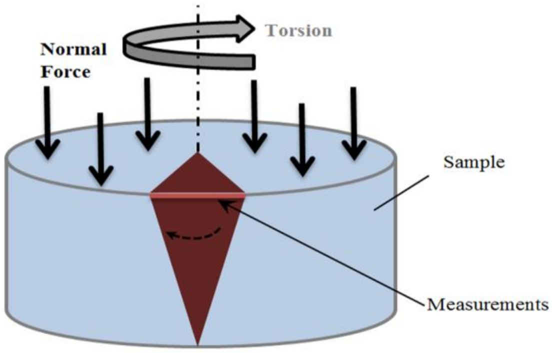

Fig. 21 Schematic diagram of forces acting on DSR sample

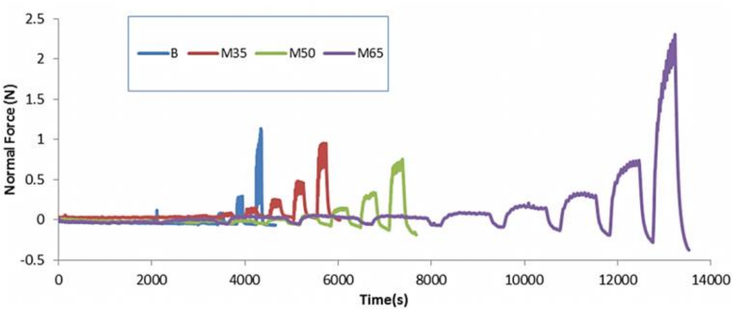

Fig. 22 Change of normal force with time in MS-SCR @40^{0}C

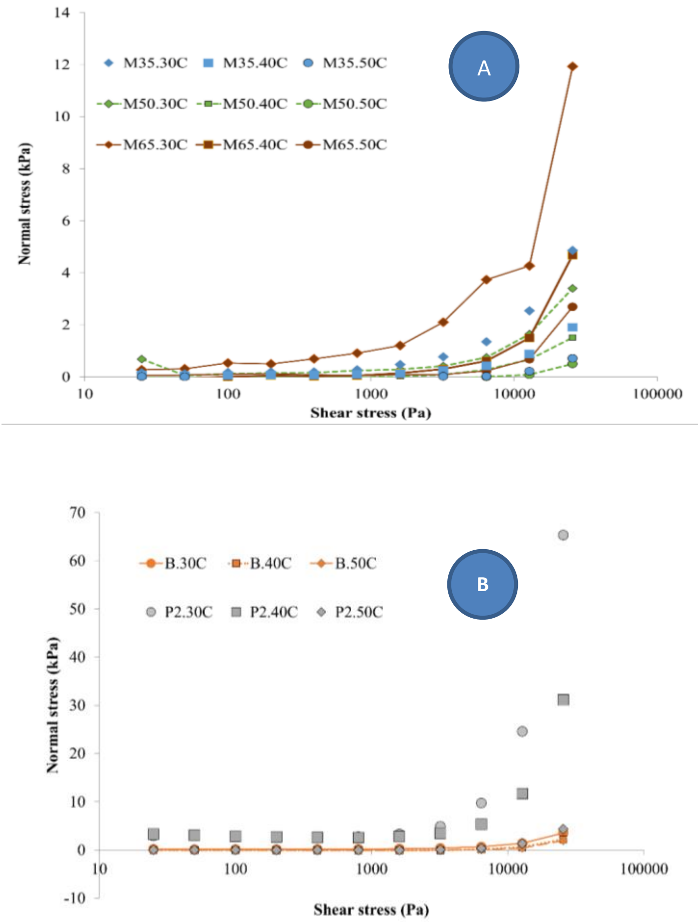

Fig. 23 Normal stress against shear stress in MS-SCR test